Materials Science Forum
ISSN: 1662-9752, Vol. 1156, pp 57-64
doi:10.4028/p-0Vb1Ug

Submitted: 2024-09-21
Revised: 2025-08-12
Accepted: 2025-08-12
Online: 2025-09-04

New Insights into the Occurrence of Prismatic Slip During PVT Growth of SiC Crystals

Shanshan Hu[1,a*], Balaji Raghothamachar[1,b], Zeyu Chen[1,c], Kevin Kayang[1,d], Dilip Gersappe[1,e], Michael Dudley[1,f], Victor Torres[2,g], Douglas Dukes[2,h], Diana Lang[2,i], Andy Martin[2,j], Hunter Briccetti[2,k], Samantha Griswold[2,l], Thomas Kegg[2,m] and Nicholas Griffin[2,n]

[1]Department of Materials Science & Chemical Engineering, Stony Brook University, Stony Brook, NY 11794, USA

[2]Pallidus, Inc., Albany, NY 12203, USA

[a]shanshan.hu@stonybrook.edu, [b]balaji.raghothamachar@stonybrook.edu, [c]zeyu.chen@stonybrook.edu, [d]kevin.kayang@stonybrook.edu, [e]dilip.gersappe@stonybrook.edu, [f]michael.dudley@stonybrook.edu, [g]victor.torres@pallidus.com, [h]douglas.dukes@pallidus.com, [i]diana.lang@pallidus.com, [j]andy.martin@pallidus.com, [k]hunter.briccetti@pallidus.com, [l]sam.griswold@pallidus.com, [m]tom.kegg@pallidus.com, [n]nicholas.griffin@pallidus.com

Keywords: X-ray topography, 4H-SiC, PVT growth, prismatic slip

Abstract. Prismatic slip systems are the secondary slip systems in Silicon carbide (4H-SiC) crystals. The previously proposed radial thermal model of the PVT growth process for SiC crystals, which predicts the occurrence of slip in different prismatic planes as a function of the radial position in the boule, has been shown to generally work well. Recent observations of growth interface nucleation of prismatic slip necessitated updating the thermal model to incorporate the effects of the curvature of the growth interface. A 3D finite element model has been developed to include the growth interface curvature complexity. The model predicts high dislocation densities due to prismatic slip near the peripheral regions dropping to zero near the center for wafers from sections of the boule grown with a flatter interface and a less dense distribution of prismatic slip dislocations that extends to the center for wafers from boule sections grown with a more convex interface. Additionally, due to such an interface-initiated prismatic slip, , the asymmetrical step configuration produced by off-axis growth results in an asymmetrical distribution of prismatic slip. The studies suggest that a reduced surface curvature is necessary to suppress the prevalence of interface-related prismatic slip generation.

Introduction

Silicon carbide (SiC) has become the material of choice for next-generation high-power electronic devices[1]. Efforts are ongoing to optimize the physical vapor transport (PVT) growth process with the goal of obtaining 150 mm wafers with reduced dislocation densities, including threading screw/mixed dislocations (TSDs/TMDs), threading edge dislocations (TEDs), as well as basal plane dislocations (BPDs). These defects negatively affect the reliability of high-performance 4H-SiC power devices, limiting their widespread adoption in power electronics[2]. SiC crystals grown by PVT possess a low density of dislocations and other structural defects. The basal plane slip system ($\{0001\}\langle 11\bar{2}0\rangle$) is the most frequently observed deformation mechanism in SiC crystals grown by PVT, while the prismatic slip systems ($\{1\bar{1}00\}\langle 11\bar{2}0\rangle$) are activated as well[3-5]. Prismatic slip occurs when threading edge dislocations (TEDs) in prismatic planes glide under the influence of radial thermal gradient stresses[6, 7]. The TED glide leaves behind screw dislocation segments which can then cross-slip onto the basal plane.

Previously, we reported on a radial thermal model of the PVT growth process developed to predict the distribution of prismatic slip[8, 9]. Based on a cylindrical boule, this model predicted the occurrence of slips in different prismatic planes as a function of the radial position in the boule. The predicted distributions showed a good correlation with observed distribution on X-ray topographs, clearly demonstrating the role of radial thermal gradients in activating prismatic slip during PVT growth. However, recent studies of X-ray topography of 4H-SiC axial wafers indicate interface-related prismatic slip nucleation at work, suggesting the current model must be updated to incorporate the effect of the growth interface curvature to describe the distribution of prismatic slip.

Experimental

Two 4° off-axis 150 mm PVT-grown 4H-SiC commercial wafers (marked as Sample A and Sample B) were sliced from the same boule. Sample A is from a later growth stage at the position further from the seed, while Sample B is from an early growth stage at the position closer to the seed. Furthermore, several axial slices cut parallel to the [0001] growth axis are prepared to image the distribution of prismatic slip dislocations with respect to the growth interface. All samples were imaged by Synchrotron White Beam X-ray Topography (SWBXT) in transmission geometry with $11\bar{2}0$ reflection and the images were recorded on AGFA Structurix D3-SC films.

Finite Element Modeling

A 3D finite element model (FEM) was developed to simulate the thermal stress distribution within the boule. The general-purpose FE modeling analysis software ABAQUS/Standard was used for these simulations[10]. The boule sample was modeled as a circular disc of radius 150 mm with an ellipsoidal surface where the surface curvature varies. The elastic modulus and Poisson ratio used for the simulation were 411 GPa and 0.16, respectively, with a coefficient of thermal expansion of $5.22 \times 10^{-6} K^{-1}$. Thermal stresses in the sample were induced due to the radial thermal gradient [8] according to:

$$T = 2400 + a \cdot log(b \cdot r + 1) \quad (1)$$

Where a and b are constants taken as $100°C/m$ and 10, respectively. Additionally, the bottom of the sample was fixed such that the sample was free to expand axially and radially only. The sample was meshed using eight-node brick elements (C3D8). The thermal stresses were analyzed in the form of the resolved shear stress distribution through the samples.

Results and Discussion

The radial thermal model[8]to predict prismatic slip established previously is deduced from the thermal stress components, σ_{rr}, $\sigma_{\theta\theta}$, σ_{zz}, induced by the radial temperature gradients, where σ_{rr} is along the radial direction, $\sigma_{\theta\theta}$ is perpendicular to both radial and growth directions, and σ_{zz} is parallel to the growth direction, as indicated by Fig. 1(a). By applying the corresponding Schmid's factor, the estimated thermal stress can resolve onto each of three prismatic slip systems. Thus, the resolved shear stress for prismatic systems can be estimated at any location in the crystal boule. For example, for prismatic system $(1\bar{1}00)[\ 11\bar{2}0]$, the resolved shear stress τ is given by:

$$\tau = (\sigma_{rr} - \sigma_{\theta\theta}) cos\theta sin\theta \quad (2)$$

Where θ is the angle between any point on the plane perpendicular to the growth axis at a height of z and $[11\bar{2}0]$ direction.

As a result, the predicted distribution of all three sets of prismatic slip systems on 4H-SiC commercial wafers can be obtained as schematically shown in Fig. 1(b). Prismatic slip is observed at the periphery regions with higher resolved shear stress. Two sets of prismatic slip dislocations are observed at each of the twelve different periphery regions around the wafer. In particular, the stress level of the resolved shear stress affects the extent to which the distribution of activated prismatic slip regions extends towards the center of the crystal and the density of prismatic slip dislocations. A higher resolved shear stress level implies prismatic slip extends further into the center of the crystal with higher density.

SWBXT transmission images recorded from the twelve different regions of Samples A and B are compared with predicted results. As shown in Fig. 1(c) for Sample A, prismatic slip dislocations can be clearly identified as straight dark lines running along one of the three $\langle 11\bar{2}0 \rangle$ directions. An excellent agreement is found between the topograph and prediction for prismatic slip distribution, generally validating the radial thermal model.

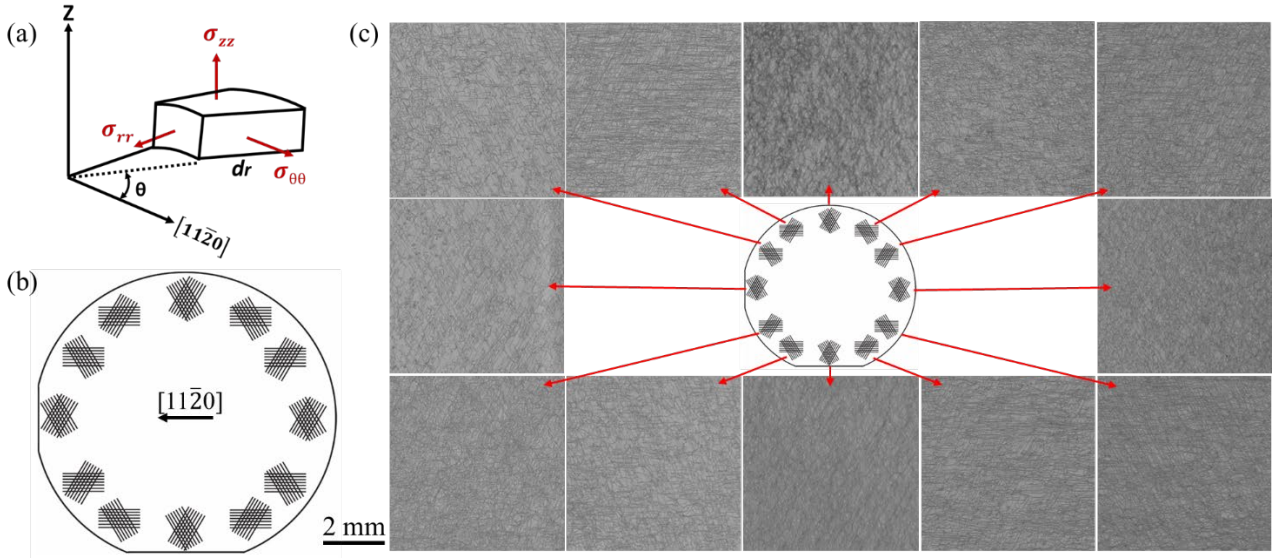

Fig. 1. (a)Coordinate system for the thermal model. (b) Predicted map indicating the distribution of prismatic slip dislocations by the radial thermal model. (b) A good correlation is observed between the SWBXT images (**g**=$11\bar{2}0$) for Sample A and the predicted map.

Analysis of the axial wafers reveals prismatic slip nucleation from the growth interface. As shown by Fig. 2(a), dislocation loops are observed to nucleate at the as-grown interface and propagate into the crystal from axial slices cut roughly parallel to the [0001] growth axis. The loops are composed of a segment approximately along the growth axis connected with two segments approximately parallel to basal planes at its two ends, suggesting they are generated by the gliding of the TED segments inside prismatic planes, leaving two segments of dislocation in its wake. Four prismatic slip half loops are observed in Fig. 2(a), as indicated by red arrows. Since the axial slice was cut along the direction close to $[11\bar{2}0]$ direction, the prismatic slip half loops are confirmed to belong to the $(1\bar{1}00)[11\bar{2}0]$ prismatic slip system. The loops have weak contrast on the topograph, and a schematic of Fig. 2(a) is constructed, as shown by Fig. 2(b), to clearly indicate the positions of prismatic slip half loops.

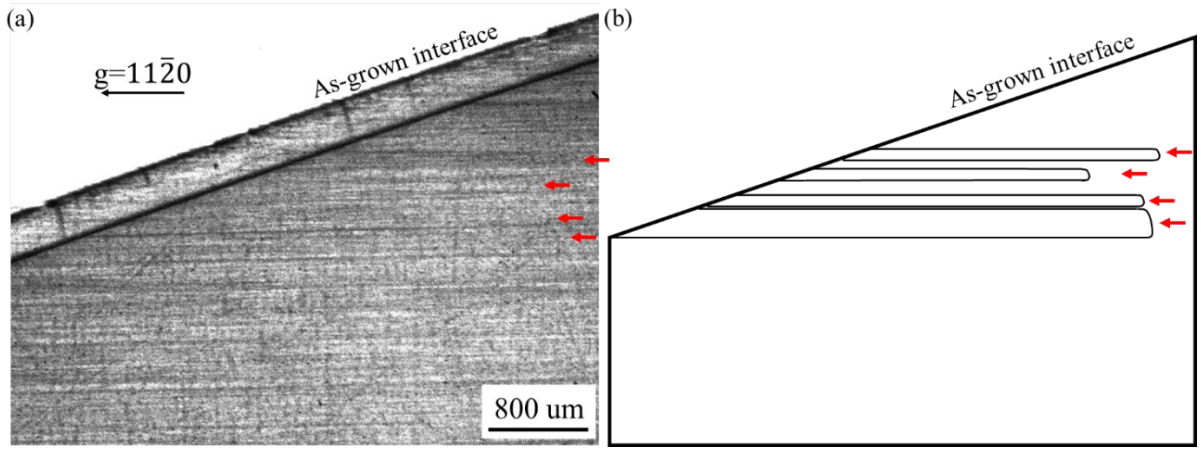

Fig. 2. (a) SWBXT image with 11$\bar{2}$0reflection recorded from an axial slice cut parallel to the [0001] growth axis showing nucleation and propagation of prismatic slip half loops from the as-grown interface as marked by red arrows, and (b) a schematic helping locate prismatic slip half loops in (a).

The previously developed radial thermal model does not take into account such surface nucleated prismatic slips. Therefore, an updated model to include the growth interface curvature complexity is developed to obtain a more comprehensive picture of prismatic slip in the boule.
A 3D FE thermal model that incorporates the shape of the interface is employed. As shown in Fig. 3, the stress distribution across the cross-section of the as-grown interface for the PVT-grown 150 mm 4H-SiC boule is suggested by the modified thermal model with a less convex interface (Fig. 3(a)) and more convex interface (Fig. 3(b)). Clearly, the less convex interface has lower stress, while the more convex interface has high stress even in the middle region of the boule, which was not predicted by the previous model.

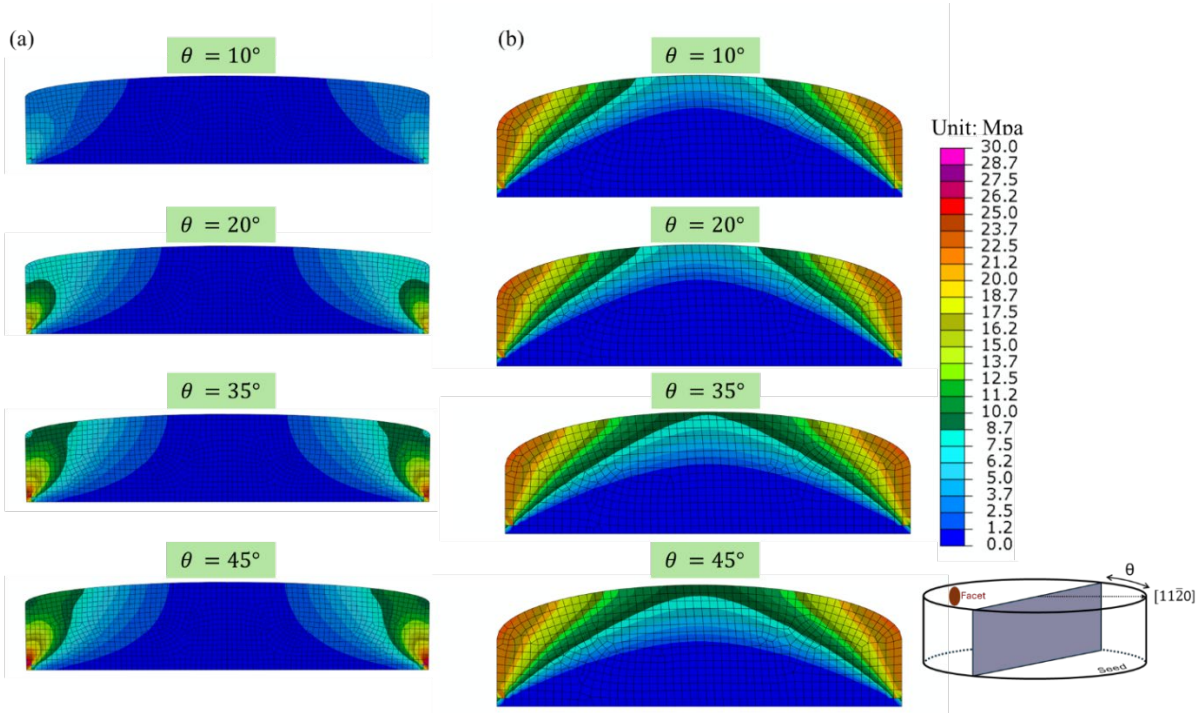

Fig. 3. Resolved shear stress distribution across the cross-section of a 150 mm 4H-SiC boule for the (1$\bar{1}$00)[11$\bar{2}$0] prismatic slip system during PVT growth obtained by finite element method for (a) less convex interface and (b) more convex interface, showing that convex interface can introduce higher stress during crystal growth even for the middle region of the boule. Cross-sectional maps are for different radial positions around the boule as indicated by the boule schematic. The same maps can also be used for the other two slip systems by rotating 60°.

The higher stresses can, therefore, induce nucleation of prismatic slip dislocation loops with a more convex-shaped interface. Fig. 4(b) and (c) show $11\bar{2}0$ transmission images recorded from Sample A and Sample B at regions 1, 2, 3, and 4, ranging from periphery regions to central regions, whose locations are shown in Fig. 4(a). As shown by Fig. 4(b), for Sample A from the later growth stage, a less dense distribution of prismatic slip dislocations extends all the way to the center as they are observed in all regions of 1, 2, 3, and 4. However, Fig. 4(c) indicates that high dislocation densities near the peripheral regions dropping to zero near the center are formed during the early growth stage, as prismatic slip dislocations are not observable in region 4 of Sample B.

The previous radial thermal model is not sufficient to explain such prismatic slip distribution difference between Sample A and Sample B. Based on that model, Sample A has a lower stress level than Sample B since Sample A has lower prismatic slip dislocation densities for regions 1, 2, 3 compared to Sample B. However, the model cannot account for the observation of prismatic slips in region 4 of Sample A and absence in region 4 of Sample B.

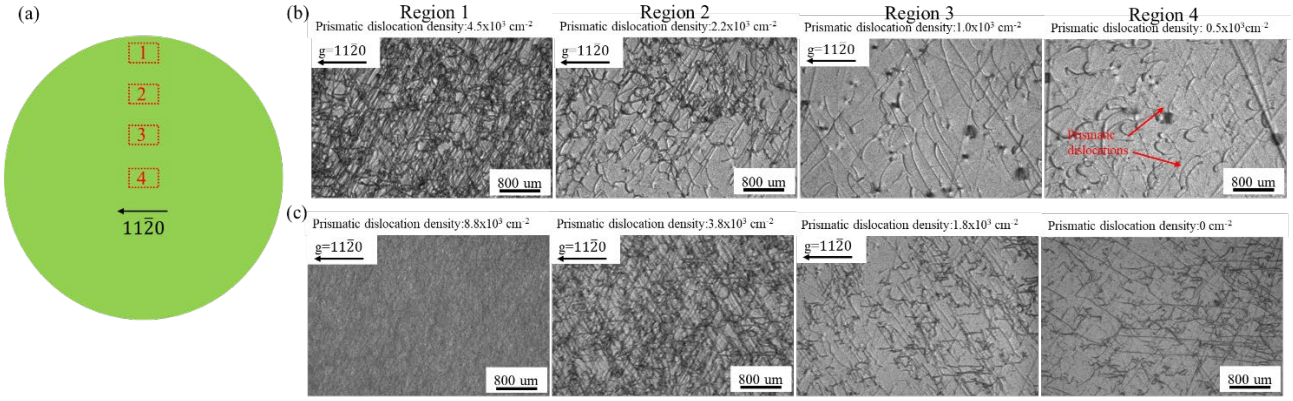

Fig. 4. (a) Approximate locations on the 150 mm substrates where x-ray topographs were recorded in four regions (1, 2, 3, and 4), and the corresponding transmission topographs with $11\bar{2}0$ reflection for (b) Sample A from later growth stage, and (c) Sample B from early growth stage. Prismatic slip dislocations protrude into region 4 for Sample A, while no prismatic slip dislocations are observed in region 4 for Sample B. Prismatic slip dislocation densities are indicated in each X-ray topograph.

The modified 3D thermal model can now be employed to explain such prismatic slip dislocation distribution in Sample A and Sample B. The interface shape during crystal growth for Sample A and Sample B can be estimated by the position of the facet on the wafer. As schematically shown by Fig. 5, the facet of Sample A is located closer to the center than that of Sample B, suggesting that Sample A has a domed interface while Sample B has a flatter interface as the facet is formed at the position where the interface is 4° away from the horizontal because of the off-cut growth. As predicted by the new model, the domed-shaped interface for Sample A introduces a higher stress level in the center, nucleating prismatic dislocation loops even at the central region of the crystal boule, while the flatter interface for Sample B does not introduce prismatic dislocation loops. The prismatic slip dislocation distribution in Sample A and Sample B thus verifies and justifies the need for the modified 3D thermal model.

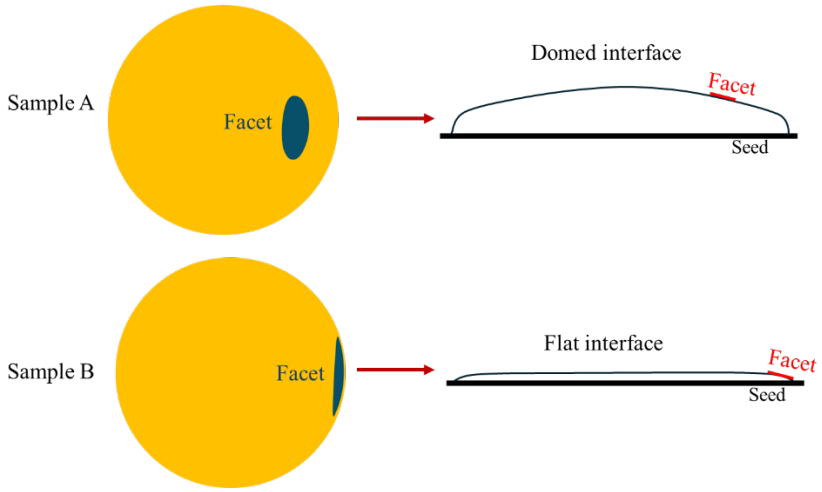

Fig. 5. Schematics showing the interface shape can be estimated by the facet position. Sample A has a domed interface, and Sample B has a flatter interface.

It should be noted that the dislocation loop nucleation at the as-grown interface is related to step configurations on the interface. As shown by Fig. 6, kinks on the vertical step risers of the macro-steps may act as sites for nucleation of half loops on prismatic planes, while the junctions between step risers and terraces can introduce BPD half loops.

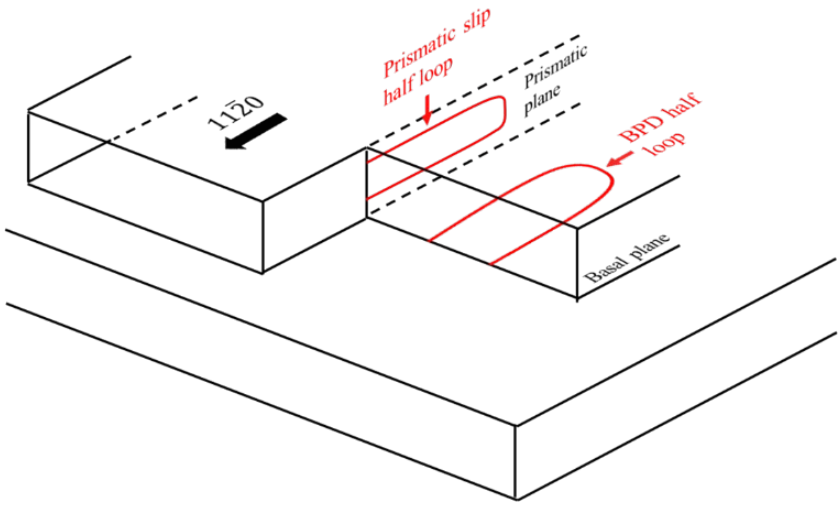

Fig. 6. Diagram schematically showing the prismatic half loops can be nucleated at the vertical step risers of the macro-steps, and BPD half loops are introduced from the junctions between step risers and terraces.

The domed and flatter interfaces have different step configurations at the as-grown interface. Fig. 7 schematically shows the cross-sectional images for the step configurations of Sample A and Sample B. As shown by Fig. 7(a), with the domed as-grown interface, Sample A has narrower terraces during crystal growth, encouraging the formation of macro-steps, especially at the position further from the facet with a larger tilt angle to the facet. The vertical step risers of the macro-steps can offer the sites for nucleation and propagation of prismatic plane dislocation half loops. Meanwhile, as indicated by Fig. 7(b), macro-steps are less likely to form on the flatter as-grown interface of Sample B, making the nucleation of prismatic plane dislocation half-loops more difficult.

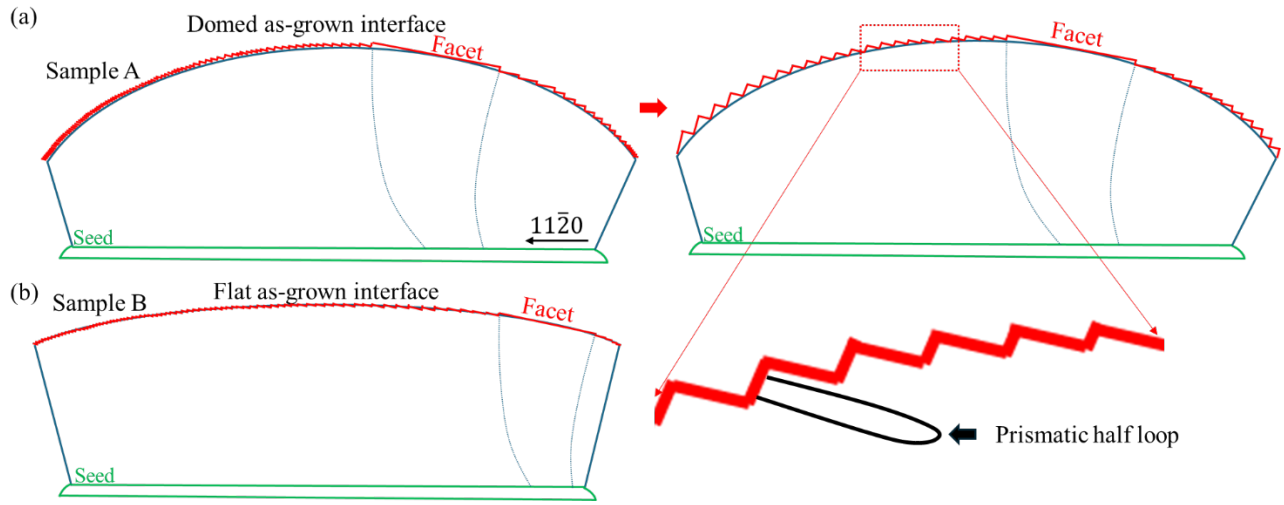

Fig. 7. Schematics showing step configurations for (a) domed as-grown interface of Sample A and (b) flatter as-grown interface of Sample B. Domed as-grown interface can encourage the formation of macro-steps, offering sites for nucleation of prismatic half loops.

From Fig. 7(a), we note that the 4° off-cut causes asymmetrical distribution of macro-steps. The left side of Sample A, which is further away from the facet, has more macro-steps, which are large compared to the right side of Sample A. This implies that more prismatic plane dislocation half-loops can nucleate on the left side than on the right side of Sample A. This prediction correlates with observation from Sample A. As shown by Fig. 8(a), when the wafer is cut from the boule of the crystal, different positions on the wafer come from different growth stages. With the domed as-grown interface, the center of the wafer comes from the earlier growth stage, while the peripheral part of the wafer comes from the later growth stage. The asymmetrical distribution of prismatic slip dislocations is observed in Sample A. As shown by Fig. 8(b), in the SWBXT image for the whole Sample A wafer, the outer regions of the wafer have a darker contrast due to the high density of prismatic slip dislocations. On the left side of the wafer, the high-density prismatic slip dislocation region protrudes further towards the center of the wafer (~4.6cm) than on the right side of the wafer (~3cm).

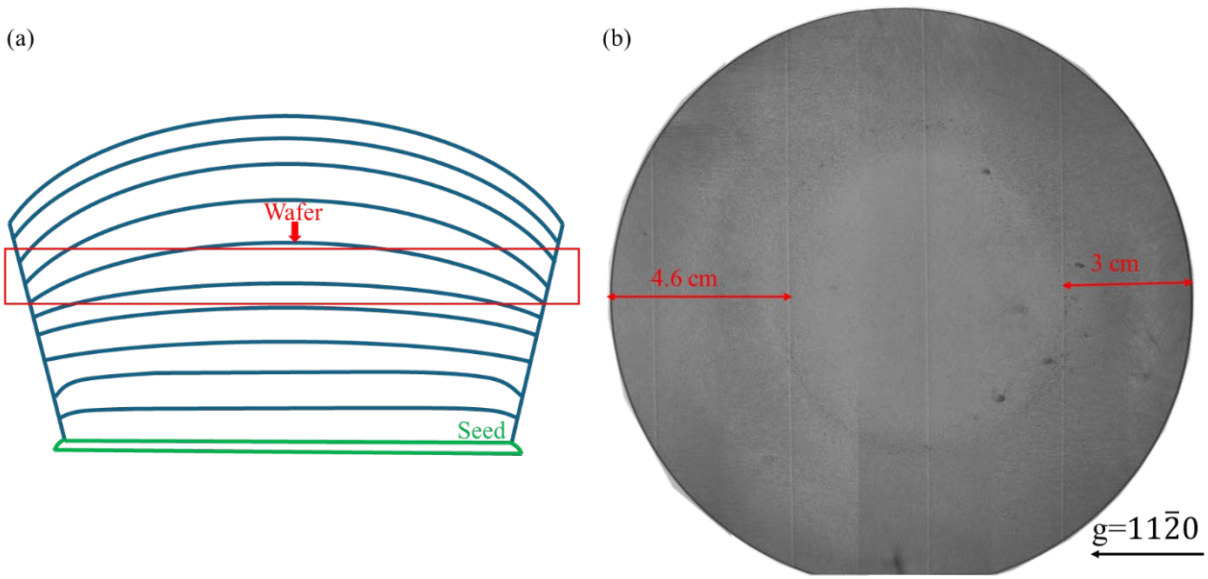

Fig. 8. (a) Schematic of the boule showing that the different positions on the wafer come from different growth stages. Domed as-grown interface makes the wafer center region come from the early growth stage, and the peripheral region comes from the later growth stage. (b) Whole SWBXT image for Sample A. The high-density prismatic slip dislocation region is wider for the left side compared to the right side, correlating with the prediction from the step configuration analysis of Sample A.

Summary

The limitations of the radial thermal model created previously for prismatic slip interpretation in PVT-grown 4H-SiC crystals are addressed by a modified 3D FEA thermal model by including the influence of as-grown interface shape on prismatic slip during crystal growth. The modified 3D thermal model helps understand the prismatic slip dislocation distribution in the central regions, as well as the asymmetrical distribution of prismatic slip dislocations on PVT-grown 4H-SiC wafers. The results demonstrate that it is necessary to control the as-grown interface shape to restrain the defect generation inside the boule during the PVT growth of 4H-SiC.

Acknowledgement

This work was supported by Pallidus, Inc.. This research used resources of the National Synchrotron Light Source II, a U.S. Department of Energy (DOE) Office of Science User Facility operated for the DOE Office of Science by Brookhaven National Laboratory under Contract No. DE-SC0012704. This research used resources of the Advanced Photon Source (Beamline 1-BM), a U.S. Department of Energy (DOE) Office of Science User Facility operated for the DOE Office of Science by Argonne National Laboratory under Contract No. DE-AC02-06CH11357. The Joint Photon Sciences Institute at SBU provided partial support for travel and subsistence for access to Advanced Photon Source.

References

[1] H. Matsunami, T. Kimoto, Step-controlled epitaxial growth of SiC: High quality homoepitaxy, Mater. Sci. Eng. R Rep. 20 (1997) 125-166.

[2] R. SIngh, M. PEchT, Commercial impact of silicon carbide, IEEE Ind. Electron. Mag. 2 (2008) 19-31.

[3] S. Ha, N. T. Nuhfer, G. S. Rohrer, M. De Graef, M. Skowronski, Identification of prismatic slip bands in 4H SiC boules grown by physical vapor transport, J. Electron. Mater. 29 (2000) L5-L8.

[4] H. H. Wang, S. Y. Byrapa, F. Wu, B. Raghothamachar, M. Dudley, E. Sanchez, D. M. Hansen, R. Drachev, S. G. Mueller, M. J. Loboda, Basal plane dislocation multiplication via the hopping frank-read source mechanism and observations of prismatic glide in 4H-SiC, Mater Sci Forum 717 (2012) 327-330.

[5] H. Wang, Studies of growth mechanism and defect origins in 4H-silicon carbide substrates and homoepitaxial layers, dissertation, Stony Brook University. 2014.

[6] S. Hu, H. Fang, Y. Liu, H. Peng, T. Ailihumaer, Q. Cheng, Z. Chen, R. Dalmau, J. Britt, R. Schlesser, Prismatic slip in AlN crystals grown by PVT, ECS Transactions 104 (2021) 57-64.

[7] S. Hu, H. Fang, Y. Liu, H. Peng, Q. Cheng, Z. Chen, R. Dalmau, J. Britt, R. Schlesser, B. Raghothamachar, Characterization of prismatic slip in PVT-grown AlN crystals, J. Cryst. Growth 584 (2022) 126548.

[8] J. Guo, Y. Yang, B. Raghothamachar, J. Kim, M. Dudley, G. Chung, E. Sanchez, J. Quast, I. Manning, Prismatic slip in PVT-grown 4H-SiC crystals, J. Electron. Mater. 46 (2017) 2040-2044.

[9] J. Guo, Y. Yang, O. Y. Goue, B. Raghothamachar, M. Dudley, Study on the role of thermal stress on prismatic slip of dislocations in 4H-SiC crystals grown by PVT method, ECS Transactions 75 (2016) 163-168.

[10] M. Smith, ABAQUS/standard user's manual, version 6.9, (2009).